Contrib. Mineral. Petrol. 75, 97–110 (1980)

Contributions to Mineralogy and Petrology

Phase Relations and Metamorphic History of a Clinohumite-Chlorite-Serpentine-Marble from the Western Tauern Area (Austria)

G. Franz[1] and D. Ackermand[2]

[1] Institut für Angewandte Geophysik, Petrologie und Lagerstättenforschung, Straße des 17. Juni 135, D-1000 Berlin 12, Federal Republic of Germany

[2] Mineralogisches Institut, Olshausenstr. 40–60, D-2300 Kiel, Federal Republic of Germany

Abstract. Several different metamorphic events – an early or prevariscian regional, a variscian contact and the alpine regional – on marbles from the Schlegeistal (Western Tauern Area, Tyrol, Austria) have resulted in a great variety of mineral assemblages. These assemblages include calcite, dolomite, tremolite, diopside, forsterite, clinohumite-titanianclinohumite-chondrodite, chlorite-serpentine, brucite, and boron minerals karlite and ludwigite.

Microprobe analysis fo the minerals indicate that three different generations of chlorite minerals exist (clinochlor, penninite, Al-serpentine). The occurence of these chlorites is explained by formation of serpentine component during the last (alpine) regional metamorphism from the breakdown of forsterite, humite-minerals and diopside. The phase relations are described in the system $CaO-MgO-SiO_2-H_2O-CO_2-HF$ and a petrogenetic grid for the low $X_{CO_2}^{fluid}$, low $X_F^{mineral}$ region is given. The reactions are typical for ophicarbonate rocks, but include clinohumite and chlorite, due to the presence of F and minor amounts of Al_2O_3.

Introduction

Phase relations in metamorphosed silica rich dolomitic limestones have been studied by many authors experimentally and by field observations over a wide range of pressures and temperatures. These studies have yielded estimates of the $P-T$-conditions of metamorphism. Reactions in the system $CaO-MgO-SiO_2-H_2O-CO_2$ are dependent upon the composition of the fluid phase (X_{CO_2}). In natural systems there is an additional influence upon the composition of the solid phases, especially F substituting OH. The marbles from Schlegeistal (Zillertal/Austria) are well suited to study this influence and a detailed petrological and mineralogical study made it possible to develop a petrogenetic grid for this natural system with minor amounts of Al_2O_3 and F present.

From a geological point of view the position of the marbles at the border zone between the variscian tonalites and the Greiner Schiefer serie is very interesting. Relic minerals give proof of an older contact metamorphism which was followed by the alpine metamorphism.

Reprint requests to: D. Ackermand

Geological Setting

The Schlegeistal area is situated in the western part of the Tauern window and belongs to the penninic zone. The map by Christa (1931) shows marble layers occuring within an amphibolite series immediately adjacent to metatonalites. These metatonalites belong to the "Zentralgneiskern (central gneiss body)-Zillertal-gneiss-core". The centralgneisscore is surrounded by the lithological unit of the Lower Schieferhülle. According to Angenheister et al. (1972) and Morteani (1974) the Lower Schieferhülle of the investigated area consists of micaschists of the Tux-Grossvenediger series (called Altkristallin series) and the Greiner-Schiefer series. The Altkristallin series is represented here by amphibolites and "injected schists", the Greiner Schiefer series by the Furtschagl-Schiefer and the Hornblendegarbenschiefer which occur further to the north of the described locality (see Fig. 1). The age of these rocks (mostly metasediments or tufficious rocks) is assumed to be paleozoic (Angenheister et al. 1972; Morteani 1974).

The age of the tonalite intrusion has not yet been determined, but age determinations of migmatites at the Berliner Hütte near to this locality (unpublished data by Satir and Morteani, in preparation) yielded ages of the migmatisation of 283 ± 28 Ma. Similar total rock ages (244 Ma) for a meta-aplite (intruded into the metatonalite of the South East Tauern window) were determined by Cliff et al. (1971). Very probably the metatonalites from the Western Tauern area have the same variscian age (Morteani 1974).

For the most part the intrusive contact between metatonalite and amphibolite is sharp and more or less parallel to the schistosity planes. However in the western part of the area (see Fig. 1) the contact has a migmatitic appearance. Pegmatitic dikes are intruded

0010-7999/80/0075/0097/$02.80

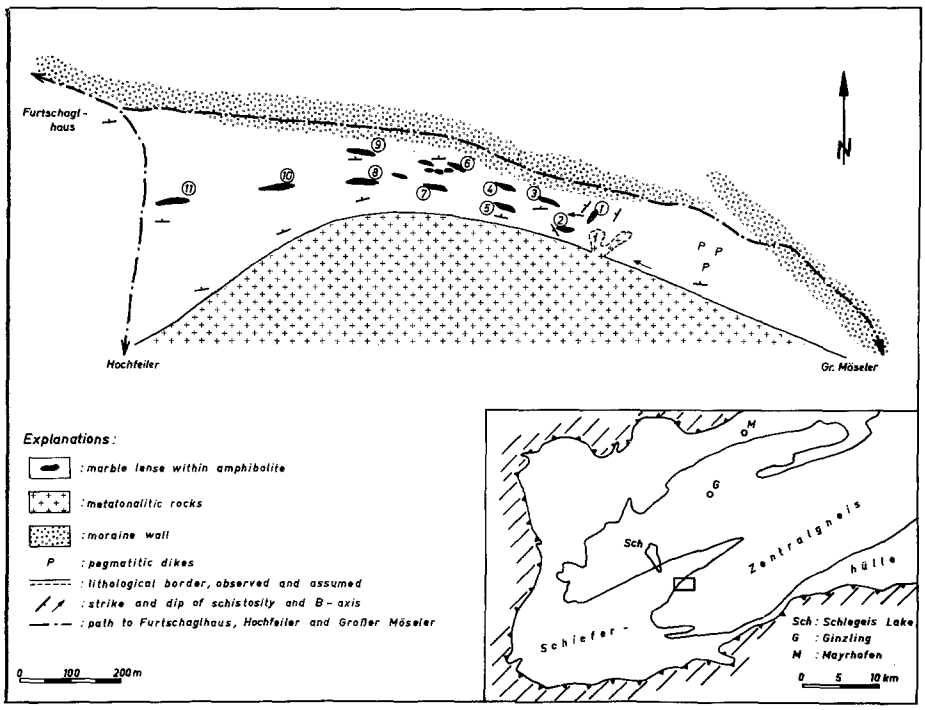

Fig. 1. Geological map fo the investigated area. *Inset* shows geographical and geological position within the western Tauern Window

into the amphibolite. The schistosity planes within different amphibolite xenoliths show random orientation; this clearly demonstrates that the migmatisation occurred when the amphibolite was already metamorphosed. Furthermore we observed aggregates of tourmaline and large mica crystals within the amphibolite as well as within the pegmatites. This indicates that boron metasomatism took place.

The dikes as well as the tonalite itself are tectonically deformed and intensely metamorphosed. This was produced by the last metamorphism which is characteristic for this part of the penninic zone. It is of alpine age and was called "Tauernkristallisation" by Sander (1911).

Approximately 20 to 50 m away from the intrusive contact 11 calcsilicate-marble lenses were mapped (see Fig. 1). These lenses are up 1 m thick, their length varying between 1 and 10 m approximately. The marbles show an intensive folded layering of white-yellowish (predominantly carbonate) and greenish (predominantly silicate) layers. Very often rounded "sponge like" forms were observed similar to those described by Tilley (1951); zoning is present in these nodules but is not always distinct.

Probably the marble formed a continuous layer which was destroyed by tectonic deformation. Its strike generally varies between N 70° to 100°E with a steep dip of about 80° in northern direction. Only in the western part values of N 40° to 50°E/50°W were measured where two small metatonalite bodies were found within the amphibolite.

Mineral Assemblages of the Marble Lenses

A total of 11 marble lenses were mapped and numbered in Fig. 1; we refer to these numbers in the tables as well as in the text. Lense No. 6 consists of several small outcrops which were described together. Other very small outcrops were not investigated. Table 1 gives a summary of the minerals observed in the marble, in the nodules (sponge like forms), at the border zones to the amphibolite, and in veins. Emphasis was placed on the mineral assemblages of the marble. The border zones and vein fillings were not investigated in detail.

Two different types of mineral assemblages exist in the marble. The first one, to which lenses Nos. 1, 2, 3, 5, 6, 7, and 8 belong, contain assemblages with the minerals:

calcite-dolomite-(titanian)clinohumite-chlorite-ludwigite (±forsterite, diopside, accessories).

Lenses Nos. 9, 10, and 11 contain assemblages with the minerals:

calcite-dolomite-diopside-tremolite-chlorite (±accessories). Lense No. 4 contains both, tremolite and ludwigite, and is therefore intermediate between these two types. In the border zones of lenses Nos. 5 and 6 tremolite is present.

In lenses Nos. 1, 4, 6, and 9 the mineral assemblages within the nodules are the same as in the marble; however, the amount of silicate minerals is higher, ludwigite is absent and accessory minerals, such as apatite are more abundant. In lense No. 3 zoisite is present in the nodule, but not in the marble.

The border zone between amphibolite and marble is sometimes similar to a chlorite schist (especially at lenses Nos. 1 and 2) as it is mapped by Christa (1931), and sometimes does not show any schistosity. In this case it contains large amounts of diopside, zoisite, and garnet. Lense No. 11 is accompanied by a small (several cm thick) brown quartzitic layer. This

Table 1. Mineral assemblages of the 11 marble lenses, the nodules, border zone to amphibolite, and in veins

Lense No.	Marble	Nodules (sponge forms)	Border zone to amphibolite/veins/remarks
1	Cc-Do-Tichu-Chl_{II}(Chl_I)-Lud (202)	Di-Cc-Chl (203, core) Fo-Tichu-Chl_{III}(Chl_{II})-Cc-Do (203)	Chl-Di-Sph-Mgt-Cc (200, 201)
2	Cc-Do-Chu-Chl_I-Lud (205)		Chl_{III}(Chl_{II})-Di-Cc-Apa-Sph (209) Chl-Di-Epi-Cc-Apa-Sph (209) in veins: Epi, Cc, Gar, Chl
3	Cc-Di-Tichu-Chon-Chl_{II}(Chl_I)-Lud-Sph Do as inclusion in Chl_I-Chl_{II} (210)	Zoi-Di-Chl-Gar (212)	in veins: Qz with inclusions of amphibole
4	Cc-Di-Tre-Chl-Lud-Sph (213) Do-Tre-Cc-Chl-Sph (213) Cc-Chl-Di-Zoi (214/1)	Zoi-Chl-Tre-Cc-Sph-Apa (214/2)	Di-Zoi-Cc (215) Di-Gar-Zoi-Cc (215) Gar-Zoi-Do (215)
5	Cc-Do-Fo-Chu-Chl_{II}(Chl_I)-Bru-Lud (216, 217) relic. periclase (?) (217)		Tre (218) Tre-Chl-Do-Cc (218)
6	Cc-Do-Fo-Tichu-Chl_{II}-Lud-Op (220) Cc-Do-Di-Fo-Tichu-Chl_{III}(Chl_{II}) (Di-Do relic., 224, 227)	Tichu-Fo-Di-Chl_{III}(Chl_{II})-Cc-Do-Apa-Ru (Di-Do relic., 225)	Chl-Di-Cc-Op (219) Tre-Di-Cc-Op (221) Tre-Ta-Chl_{III}-Do-Mgt (222) Chl-Tre (223) in veins: Di-Chl-Cc (226)
7	Cc-Do-Fo-Chu-Chl_I-Lud (230, 231)		Epi-Gar-Chl-Cc (229)
8	Cc-Do-Fo-Chu-Chl_I-Bru-Lud-Ka (232)		fluorescent in veins
9	Cc-Do-Di-Tre-Chl_{III}(Chl_{II})-Phl-Apa (Di-Do-relic., 241)	Di-Chl_{III}(Chl_{II})-Cc-Phl-Apa-Op (241)	
10	Cc-Di-Tre-Chl_I (242)		
11	Cc-Do-Tre-Chl_{III}(Chl_{II})-Sph (244, 245)		cm thick brown quartzitic layer (Qz-Di) beside marble

Abbreviations: Apa = apatite; Bru = brucite; Cc = calcite; Chu = clinohumite; Chl = chlorite (type I, II, III); Chon = chondrodite; Di = diopside; Do = dolomite; Epi = epidote; Fo = forsterite; Gar = garnet; Ka = karlite; Lud = ludwigite; Mgt = magnetite; Op = opaque phases; Phl = phlogopite; Qz = quartz; Ru = rutile; Sph = sphene; Ta = talc; Tichu = titanclinohumite; Tre = tremolite; Zoi = zoisite; number of sample in brackets

quartzite consists of quartz and diopside. Apart from this, quartz as well as epidote, garnet, chlorite, diopside and calcite were found as vein fillings.

Microscopic Description of the Minerals and Mineral Chemistry

Phases from the humite group and from the chlorite group exhibit the most interesting phenomena, in terms of crystal chemistry and from their implications in the phase relationships. Therefore their description is given first, and a brief description of the other phases follows.

Clinohumite-Titanianclinohumite-Chondrodite

Minerals of the humite group (general formula $n M_2SiO_4 \cdot M_{1-x} Ti_x (OH,F)_{2-2x} O_{2x}$ where n is 4 for clinohumite and 2 for chondrodite) occur in various amounts in all of the marble lenses except the tremolite bearing ones Nos. 9, 10, and 11, which are situated in the western part of the investigated area at a greater distance from the metatonalite/amphibolite contact. Locally they are enriched in layers or in nodules and can be distinguished microscopically as yellow or brown crystals. They are also found in the border zone to the amphibolite together with pyroxene and chlorite.

Microscopically the crystals exhibit a number of different habits. Colour varies from colourless to yellowish to dark yellow with distinct pleochroism. Euhedral crystals are not observed but subhedral rounded ones which are free from inclusions are present as well as large anhedral porphyroblasts which contain numerous inclusions. The clinohumites of sample No. 225 from a nodule show cyclic twinning of up to 5 individuals (see Fig. 2). The crystals in the center of the complex twin are dark yellow whereas the outer crystals are colourless.

The humite minerals were distinguished by microanalytical and by X-ray methods. The results are summarized in Table 2. Clinohumite and its variety titanianclinohumite are the members of this group, which were frequently identified in these samples. In one sample chondrodite is present.

The clinohumites show large variations in composition. TiO_2 contents vary from 0.25 to almost 5.0 wt.%. We distinguish two groups: one group contains less than 1.5 wt.% TiO_2 (samples Nos. 205, 217, 230, and 232) and the other, which we call titanianclinohumites, contains between 2.5 and 5.0 wt.% TiO_2 (samples Nos. 203, 210, 224, 225, and 227). Jones et al. (1969) give a value of 1.9 wt.% Ti (=3,17 wt.% TiO_2) below which no relationship between F and Ti content is evident. At higher Ti-content little or no F is present, and they suggest that there may be a structural

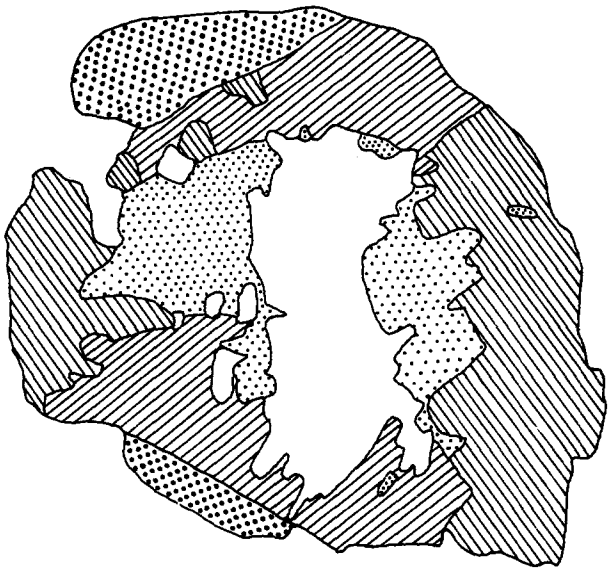

Fig. 2. Complex twinning of clinohumite (sample 225); crystals in the centre (*white* and *dotted*) are dark yellow to yellow, others (*hatched* and *heavily dotted*) are colourless (see Table 4 for comparison of yellow – the first – and colourless – the second – analyses of sample 225). The crystals are surrounded by calcite, chlorite, and other clinohumite individuals. Size of the crystal (longest diameter) is 2.9 mm

reason for this. Our data are consistent with this pattern. Titanian-clinohumites with more than 1.5 wt.% TiO_2 do not contain more than 0.3 wt.% F. All other clinohumites cluster near low Ti-contents with F-contents between 0.3 and 0.7 wt.%.

In sample 210 clinohumite was found in addition of chondrodite. This is another occurrence of coexisting clinohumite and chondrodite (see Aoki et al. 1976; Ribbe 1979) and here again we observe a Ti/Si ratio in chondrodite exactly twice as that for clinohumite (0.054–0.027). This supports Ribbe's view (1979) of completely ordered Ti-distribution into the M (3) sites of the humite minerals.

In Fig. 3a we present clinohumite (and chondrodite) analyses in a concentration triangle $TiO_2-MnO-F$. The diagram shows the relationship between F- and TiO_2-contents; clinohumites have high and titanian clinohumites have low F-contents. There is no influence of MnO (and FeO, not represented here) on F-contents.

Figure 3b shows the variation of TiO_2 content with MgO and FeO. With higher Ti values the content of FeO rises. Titanian-clinohumites show a greater variation in FeO-content than clinohumites. In thin section, titanian-clinohumites are generally more intensively coloured than clinohumites, but this is not always true. Sample No. 225 (see Fig. 2) has twinned titanianclinohumites which are partly colourless and partly dark yellow; both have high FeO (and TiO_2) contents. Sample No. 205 contains small untwinned crystals with low FeO and TiO_2 values which are partly colourless and partly yellow.

H_2O-content could not be determined but is necessary for calculating mineral formulas. Therefore, it was calculated according to the method developed by Jones et al. (1969):

$$OH=(2/(2n+1))M_{Ti}-2Ti-F$$

where n is 4 for clinohumite and 2 for chondrodite (according to the general formula of the humite minerals, see above) and M_{Ti} the atomic proportion of octahedral cations in the Mg_2SiO_4 part (=olivine part) of the formula.

The sum of microanalytically measured oxide-wt.% and calculated H_2O wt.% does not always come near to 100%, especially

Table 2. *Clinohumite and chondrodite;* representative microprobe analyses, structural formulare calculated on the basis of 4Si (clinohumite) and 2Si (chondrodite)

Lense Nos.	1	3	3	5	6	8
Sample Nos. Oxides wt.%	203/1+2	210	210	217	225	232/3
SiO_2	37.9	35.0	37.1	37.4	37.0	38.1
TiO_2	4.01	4.59	2.53	1.42	4.47	0.42
Al_2O_3	0.01	0.03	–	–	–	–
Cr_2O_3	0.01	0.01	0.02	–	–	–
FeO[a]	2.00	3.47	3.85	1.03	5.51	0.72
MnO	0.50	0.09	0.06	0.14	0.34	0.10
MgO	53.2	52.4	52.2	57.0	49.4	56.3
CaO	0.01	0.24	0.17	0.03	0.07	0.06
K_2O	–	–	–	–	–	–
Na_2O	0.01	0.01	0.03	–	–	–
F	0.13	1.11	0.90	0.82	0.29	0.14
Cl	–	0.03	–	–	–	–
	97.8	96.9	96.8	97.8	97.5	95.8
OH_{calc}	3.46	6.64	3.34		3.03	5.03
[b]tot	99.60	99.99	98.26	97.88	99.05	98.44
S[c]	1.011	1.032	1.004	1.019	1.007	1.009
Si	4.0	2.0	4.0	4.0	4.0	4.0
Mg_{oli}[d]	7.681	3.657	7.587	8.193	7.402	7.842
Fe^{2+}	0.176	0.166	0.347	0.092	0.494	0.063
Mn	0.044	0.004	0.005	0.013	0.031	0.009
Ca	0.001	0.015	0.019	0.006	0.008	0.007
oli	8.082	3.842	7.958	8.304	7.935	7.921
Ti	0.318	0.197	0.205	0.114	0.363	0.033
Mg[e]	0.682	0.803	0.795	0.886	0.637	0.967
F	0.043	0.201	0.307		0.099	0.047
OH	1.297	1.340	1.272	–	1.158	1.867
O[f]	0.660	0.459	0.428	–	0.743	0.086

[a] Total Fe as FeO or Fe^{2+}
[b] Total, less O for F and OH
[c] stoichiometric ratio $2Si/2nM_{Ti}$ $(2n+1)$
[d] $Mg_{oli} \triangleq Mg$ in the "olivine-part" of the formula
[e] rest of Mg in the "brucite-part" of the formula
[f] $2-n_{OH}-n_F=n_O-2n_{Ti}$

in samples Nos. 205, 224, and 230 where the total sum is only 96 to 97 wt.%. It may be considered that the calculated value of H_2O does not correspond to the real H_2O value. This means that the phases are non-stoichiometric or that the analysis is wrong. However, Jones et al. (1969) gave proof of the high reliability of microprobe analysis for humite-minerals. Stoichiometry can be checked by the following ratio (Jones et al. 1969):

$$2Si:(2n/(2n+1))M_{Ti}$$

where Si is the atomic proportion of Si, and M_{Ti} the sum of atomic proportions of all octahedral cations including Ti.

The theoretical value for stoichiometry should be 1, the calculated ones vary from 0.98 to 1.03 and are independent from the total sum. Therefore the large deficiency of 100 wt.% can not be explained by non-stoichiometric crystals. Another possibility

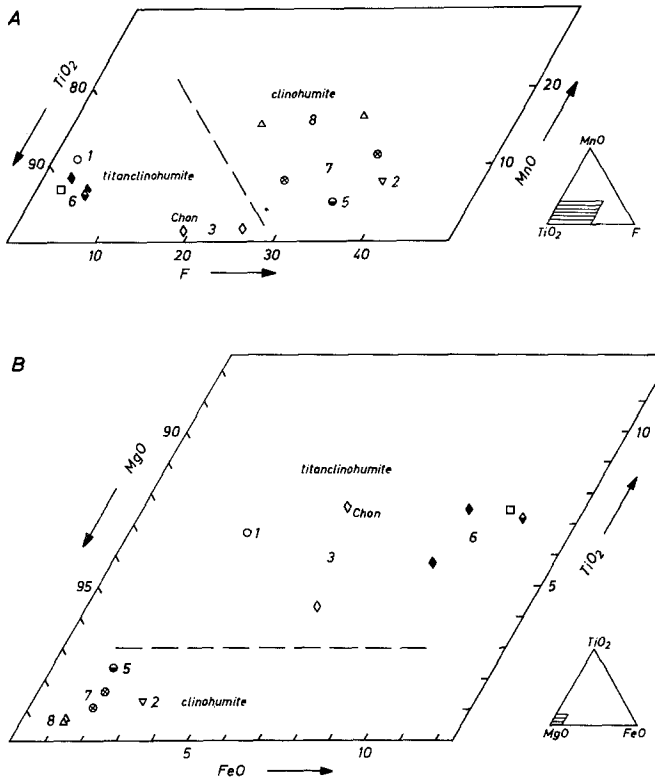

Fig. 3A and B. Parts of the systems $TiO_2-F-MnO$ (**A**) and $MgO-FeO-TiO_2$ (**B**) showing the plots of analyses of clinohumite (and one chondrodite).
A This type of diagram (plot against a minor element MnO that shows no systematic variation) demonstrates that high F content corresponds to lower Ti content. **B** Fe substitution (for Mg) is more significant in titanian clinohumites than in clinohumites. Numbers are those of the corresponding lense

for explaining the deficiency might be the incorporation of elements which cannot be measured routinely by electron microprobe, such as boron or beryllium. Boron was observed in minerals of the humite group by Hinthorne and Ribbe (1974) and these authors suggest the substitution $Si=B+OH$. BeO was observed in humites as well (see Jones et al. 1969 for references). Incorporation of B might be possible here because other B-minerals like ludwigite are present in all of the samples.

Clinohumite- and chondrodite formulas were calculated on the basis of 4 and 2 Si, respectively. Octahedral coordinated cations were separated into two groups, the "olivine-part" with the M(1)- and M(2)-sites of the formula and the "brucite-part" with the M(3)-sites. Ti was placed completely into the M(3)-sites, Fe^{2+}, Ca, and Mn^{2+} into M(1) and M(2), and Mg was put into both parts. This procedure was followed for the clearness of the formula, although Fe^{2+} is distributed more or less evenly among the three sites with a slight enrichment in M(3) (Fujino and Takeuchi 1978).

Chlorite is a characteristic mineral of all marble lenses, and is often a main component. It is colourless and can therefore easily be misidentified macroscopically as white mica. The crystals are subhedral and reach a size of 1 mm. They have blue-grey, sometimes brown interference colours. Chemical analysis (see Table 3 and Fig. 4) classifies the chlorites as serpentine-penninite-clinochlore (nomenclature according to Deer et al. 1962). Al_2O_3 content of the chlorite varies from 2.5 and 18 wt.%. FeO contents are between 1.5 and 2.5 wt.%, only in sample No. 241 were higher FeO contents of 4% observed. Fluorine contents go up to 0.17 wt.%, but many of the chlorites do not show detectable amounts of fluorine. The graphical representation of Fig. 4, where Al in tetrahedral coordination is plotted against Al in octahedral coordination, makes it evident that three types of chlorites exist: chlorite I is a clinochlore – penninite with the highest Al-contents. Chlorite II is a pure penninite with intermediate Al-contents and chlorite III has only 2 to 3 wt.% Al_2O_3. X-ray data show that these minerals belong to the 7 Å layer type but a definitive classification of serpentine type cannot be given.

Chlorite I is the first generation of chlorite. It either forms euhedral plate crystals or the core of large crystals (see Fig. 5a), which are surrounded by chlorites of generation II (Chl II). In this case only it is possible to distinguish these two chlorites microscopically, whereas the third generation, Al-bearing serpentine, can be distinguished by its typical blue interference colours. Generation III forms rims around generation II as well as interstitial grains between carbonate. Textural relationships (see Fig. 5b) show, that these serpentines are not formed by a late hydrothermal alteration (serpentinization of forsterite) of the rock, but are stable constituents of the last metamorphic assemblage. In general chlorite II and III are more rich in Fe^{2+} than chlorite I.

In lense No. 5 chlorite has the highest Al-content of all observed chlorites: correspondingly, chlorite II of this same lense has the highest Al-content of generation II. Nothing is known about a miscibility gap between penninite and clinochlore and chlorites I and II are obviously members of a continuous solid solution series. The fact that they did not equilibrate to form one single homogenous chlorite is an important hint for the reconstruction of the petrological evolution of the rock. Chlorite II and III are definitely not members of a solid solution series, since chlorite III belongs to the 7 Å-layer group and may be regarded either as an Al-serpentine or a 7 Å-chlorite.

X-ray identification of the chlorites reveal that some of them (samples 205, 218, 220, 224) show abnormal intensity ratios of basal reflections. (001) and (002) reflections are very weak compared to the data of Brown (1956), Borg and Smith (1969); reflections of higher order have comparable intensities.

Calcite is the main mineral in all of the marble lenses. It is a Mg-rich calcite with 1.13–2.19 wt.% MgO correspondig to 5 to 10 mol% dolomite. These values are consistent with data that were obtained by the X-ray methods of Goldsmith et al. (1955).

Dolomite is present in nearly all of the marbles in varying amounts. Ankeritic domolite was observed in the border zone of one of

Table 3. *Chlorite:* representative microprobe analyses, structural formulae on the basis of 56 Kat. valences

Lense Nos.	1	6	6	6	7	8	9	9
Sample Nos.	203/1	224	225	227	231	232/1	241/1	241/1
Chl-type	I	II	III	II	I	I	II	III
Oxides wt.%								
SiO_2	30.9	34.0	41.5	34.0	32.3	30.5	32.8	41.9
TiO_2	0.04	–	0.02	0.02	–	–	0.02	0.01
Al_2O_3	17.3	13.0	3.38	12.6	15.8	18.0	13.2	2.48
Cr_2O_3	–	–	–	–	–	0.01	–	–
FeO[a]	1.39	2.53	2.28	2.34	1.99	0.97	4.18	3.34
MnO	0.03	–	0.05	0.01	–	0.01	0.03	0.05
MgO	34.6	35.3	38.9	36.2	35.3	34.9	34.5	38.1
CaO	0.05	0.09	0.03	0.06	0.09	0.14	0.03	0.08
F	–	0.17	0.06	0.05	–	–	–	–
Cl	–	–	–	–	–	–	–	–
	84.3	85.0	86.3	85.5	84.5	84.5	84.7	85.9
Mg	9.929	10.099	10.883	10.327	10.021	9.981	9.994	10.752
Fe[a]	0.224	0.406	0.358	0.347	0.317	0.156	0.680	0.529
Mn	0.005	–	0.008	0.002	–	0.002	0.005	0.008
Ca	0.010	0.019	0.006	0.012	0.018	0.029	0.006	0.016
Al VI	1.892	1.473	0.557	1.351	1.710	1.933	1.414	0.484
VI	12.060	11.997	11.812	12.066	12.066	12.101	12.099	11.789
Al IV	2.034	1.469	0.192	1.496	1.843	2.143	1.622	0.069
Si	5.966	6.531	7.808	6.504	6.157	5.857	6.378	7.931
Ti	0.006	–	0.003	0.003	–	–	0.003	0.001
Fe/(Fe+Mg)	0.022	0.039	0.032	0.035	0.031	0.015	0.064	0.047

[a] Total Fe as FeO or Fe^{2+}; Na_2O and K_2O near or lower than 0.01 wt.%

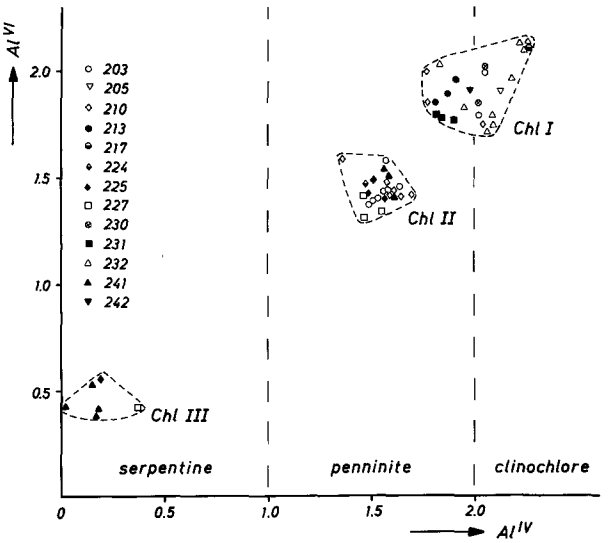

Fig. 4. A variations diagram for the clorites in which is plotted Al^{IV} against Al^{VI}. Three different generations of chlorites can be distinguished: *Chl I:* penninite-clinochlore; *Chl II:* penninite; *Chl III:* Al-serpentine

the small lenses, No. 6, together with magnetite, antigorite, tremolite and talc.

Olivine (forsterite) with a FeO-content between 1.2 and 2.3 (6.0) wt.% was observed in lenses Nos. 1, 5, 6 and 7 (see Table 4). Mean fayalite content is therefore only 2 mol%. MnO-contents are lower than 0.5 wt.% corresponding to a tephroite content of less than 0.5 mol%. It should be noted that the olivine crystals do not contain significant amounts of TiO_2, even if they occur besides Ti-clinohumite. Serpentinization of the forsterite can be observed but is not very distinct; these serpentine minerals can easily be distinguished from the serpentines of generation III (see above).

Pyroxene analyses of the marble lenses and nodules are given in Table 4. They are diopsides with a very low FeO content, which is in most cases well below 1 wt.% corresponding to a hedenbergite component of less than 1 to 2 mol%. Al_2O_3 values are mostly one order of magnitude less than FeO-contents. The pyroxenes show a remarkably F-content of up to 0.06 wt.%. A similar F-content in diopside-hedenbergite is published in analysis No. 30, Deer et al. (1963) and by Shaw et al. (1963), Magnusson (1940), and Gold (1966). In samples Nos. 224 and 241 we found large blasts of pyroxene with oriented single crystal intergrowths of calcite. The blasts are round and are up to 5 mm in diameter, sometimes surrounded by a rim of chlorite.

Tremolite is associated with diopside, calcite, dolomite, chlorite and mica in the lenses Nos. 9, 10 and 11; only in lense No. 4 was it observed together with clinohumite. Tremolite is present in the border zones of lenses Nos. 5 and 6. It occurs mostly as euhedral prismatic crystals, up to one cm long, colourless to greenish. Inclusions are frequent and consist of diopside and carbonate.

Tremolites of the border zone from lense No. 6 show zoning, where a homogeneous core is surrounded by a small rim. The rim has a seam of talc. Large crystals of tremolite are broken

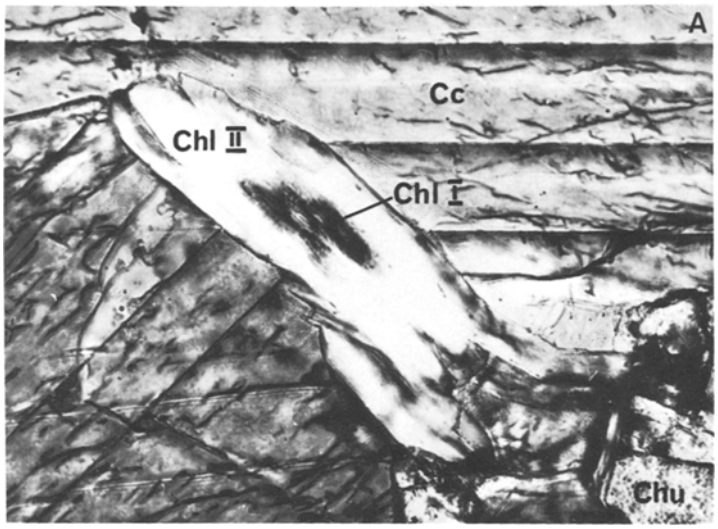

Fig. 5A and B. Microscopic pictures showing different generation of chlorite. Micrographs taken with partially crossed nicols.
A Chlorite grain (sample 210) with a core of *Chl I* (a penninite-chlinochlore) and a rim of *Chl II* (Al-poorer penninite). Size of the crystal is 0.2 mm.
B Chlorite grain of sample 227 showing Chl II (*dark*) and Chl III (*light*). Length of the picture is 0.3 mm

by tectonic movement and fractures are filled with a fine grained mass of talc, carbonate and opaque minerals.

Analyses of tremolites are compiled in Table 4. Like olivine and diopside the tremolites are poor in FeO, mostly below 1 wt. %, and contain only small amounts of Al_2O_3, approximately 0.5 wt. %.

Talc was found as a reaction product of tremolite together with ankeritic dolomite in the border zone of lense No. 6 (see Fig. 6).

Mica (Phlogopite) occurs only rarely in lense No. 9. It was observed within the marble as well as within the silicate rich nodules.

Brucite is limited on sample Nos. 217 and 232 from lenses Nos. 5 and 8. The crystals form coarse flakes which are often intergrown with smaller, mostly bent crystals of chlorite subparallel to (001). In sample 217 brucite has a reaction rim that consists of very fine grained brucite and an isotropic phase with high refractive index in the central part of this rim (together with minor amounts of opaques). This rim was too small for quantitative microprobe analysis, but qualitative analysis showed MgO as the only major oxide. Therefore it probably is periclase. *Ludwigite* and *karlite*, a new mineral from this occurrence, are described in another paper (Franz et al. 1980).

Description of Phase Relationships

The main components forming the minerals of the marble lenses are CaO, MgO, TiO_2, SiO_2, Al_2O_3, B_2O_3, CO_2, H_2O, and HF. The analyses of the different minerals show, that FeO substitutes for MgO in minor amounts only (olivines for example are 98% forsterite), hence these components can be grouped together. B_2O_3 is present only in ludwigite in most of the lenses (an exception is lense No. 8, where karlite is another borate phase) and does not influence the phase relationships. The possibility, that B_2O_3 might be incorporated in clinohumite is neglected here. Fluorine substitutes for (OH) in all (OH)-bearing

Table 4. Representative microprobe analyses of olivine, clinopyroxene and amphibole and their structural formulae

	Olivine			Clinopyroxene (diopside)			Amphibole (tremolite)		
Lense Nos.	1	5	6	1	2	4	4	9	10
Sample Nos. Oxides wt.%	203/1+2	217	220	203/2	210	213	213	241/1, 241/2	242
SiO_2	42.2	43.0	42.0	55.0	55.0[b]	53.1[c]	57.1	58.31	57.4
TiO_2	0.03	–	–	0.02	0.01	0.20	0.04	0.04	0.02
Al_2O_3	–	–	–	0.03	0.01	1.78	0.49	0.26	0.86
Cr_2O_3	–	0.02	–	0.02	0.02	0.03	0.01	0.02	–
FeO[a]	2.08	1.19	2.27	0.23	0.41	0.80	0.86	1.27	0.84
MnO	0.50	0.25	0.17	0.10	0.02	0.05	0.02	0.04	0.03
MgO	54.4	55.1	54.8	17.8	17.7	16.7	23.1	23.4	22.9
CaO	0.03	0.04	0.08	26.5	26.5	26.0	13.7	13.9	13.7
K_2O				–	–	0.01	0.05	–	0.01
Na_2O				0.01	–	0.05	0.13	0.03	0.19
	99.2	99.6	99.3	99.7	99.7	98.9	95.5	97.2	96.0
Formulae based on	8 kat. val.			12 kat. val.			46 kat. val.		
Si	1.006	1.016	1.001	1.996	1.999	1.951	7.950	7.981	7.947
Al				0.001	–	0.049	0.050	0.019	0.053
							8.000	8.000	8.000
Al				–	–	0.028	0.030	0.023	0.087
Ti				0.001	–	0.006	0.004	0.004	0.002
Mg	1.934	1.938	1.948	0.965	0.956	0.917	4.796	4.778	4.726
Fe^{2+}	0.042	0.024	0.045	0.007	0.012	0.025	0.100	0.145	0.097
Mn	0.010	0.005	0.003	0.003	0.001	0.002	0.200	0.005	0.004
	1.988	1.968	1.998	0.976	0.969	0.978	4.932	4.955	4.916
Na				0.001	–	0.004	0.035	0.008	0.051
Ca				1.029	1.031	1.025	2.049	2.032	2.038
K				–	–	–	0.009	–	0.002
				2.006	2.000	2.007	2.093	2.040	2.091
Fe/(Fe+Mg)	0.021	0.012	0.023	0.007	0.012	0.027	0.020	0.029	0.020

[a] Total Fe as FeO or Fe^{2+}
[b] $F=0.02$
[c] $F=0.06$ wt.%

phases and leads to the formation of clinohumite (chondrodite) besides forsterite. In the graphical representation HF is treated, therefore, like H_2O (and CO_2). The presence of TiO_2 leads to the formation of titanian clinohumite (with up to 4.5 wt.% TiO_2 in these samples). Other Ti-minerals like rutile or sphene are present in small amounts only and no textural relationship like those described by Trommsdorff and Evans (1980) were observed. Therefore the influence of TiO_2 on the phase relationships is neglected here, but it must be kept in mind, that Ti-substitution in clinohumite enhances its stability with respect to pure clinohumite (Trommsdorff and Evans 1980).

These simplifications allow the presentation of the parageneses of the marble in the tetrahedron $CaO-(MgO+FeO)-SiO_2-Al_2O_3$ for the condition

$P_f = P_{H_2O} + P_{CO_2} (+ P_{HF})$ (see Fig. 7).

Chlorites are the most important Al-bearing phases. Tremolite may contain small amounts of Al_2O_3 and is the only quaternary phase, but the highest Al-content (sample No. 242) is well below 1 wt.%. Therefore

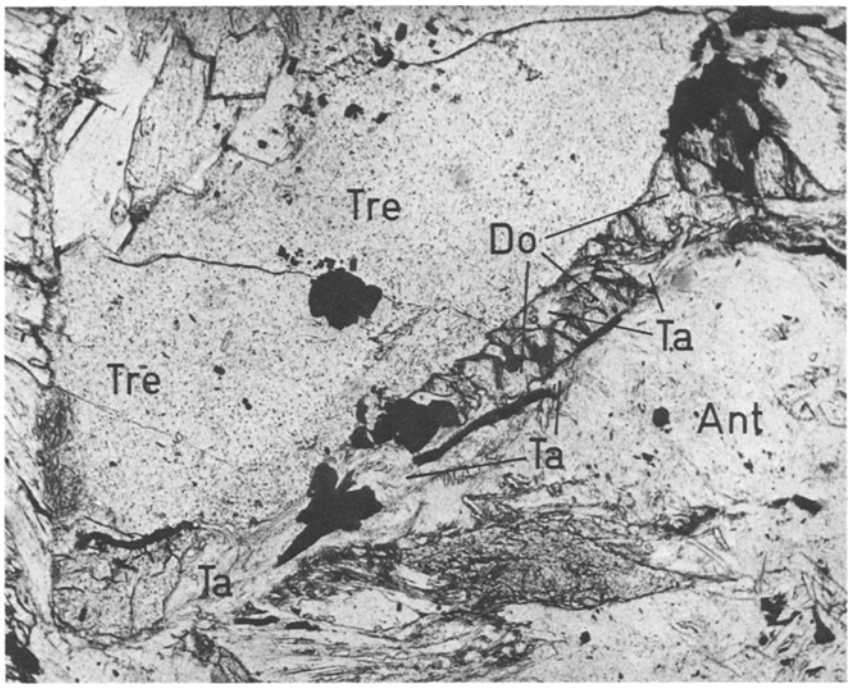

Fig. 6. Microscopic picture (sample 222) of reaction between tremolite and antigorite to form talc and dolomite. Magnetite is present, too, and the dolomite is anceritic. Length of the picture is 0.35 mm

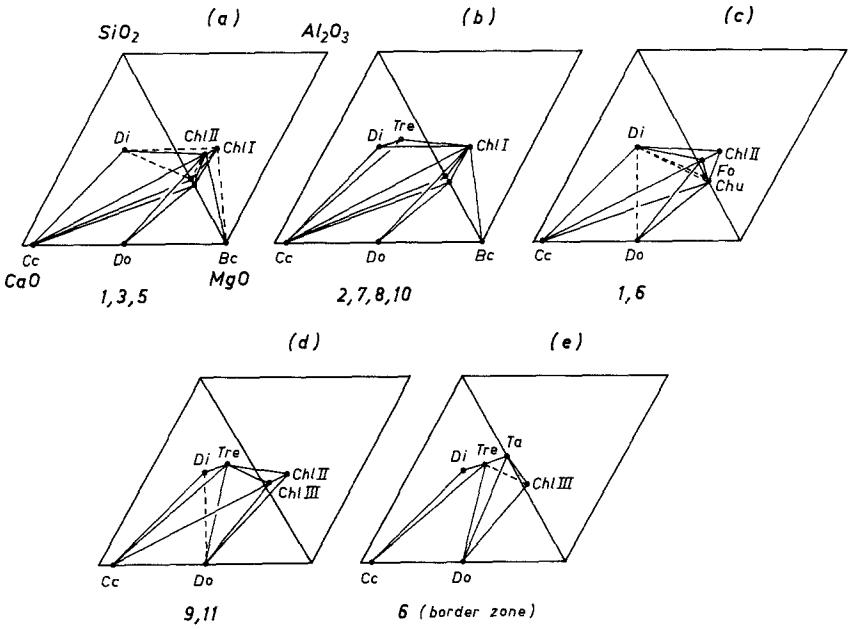

Fig. 7a–e. Phase relations of the marble lenses, represented in the tetrahedron $SiO_2-CaO-(MgO+FeO)-Al_2O_3-(+H_2O+CO_2+HF)$.
a to **e** shows the various assemblages which were formed during the last metamorphism. The arrangement is in the order of rising $X_{CO_2}^{fluid}$ and/or decreasing $X_F^{mineral}$ from **a** to **e**. *Dashed lines* indicate earlier assemblages, now preserved as relics

tremolite is placed on the $CaO-(MgO+FeO)-SiO_2$ plane. Zoisite/clinozoisite and grossularite are the phases which plot onto the $CaO-Al_2O_3-SiO_2$ plane, but they occur only in nodules and the border zones and no reactions among these phases are described. In Fig. 7 the tetrahedron is opened into the double triangle $CaO-(MgO+FeO)-SiO_2$ and $(MgO+FeO)-SiO_2-Al_2O_3$ (phase diagrams a to e).

Microscopic observation as well as the representation of the parageneses show that the Furtschagl marble does not represent equilibrium parageneses. Mineral reactions as well as different generations of phases are frequent. The most striking example is the presence of three different types of chlorite minerals. The representative points of generation I, II and III in the triangle $(MgO+FeO)-SiO_2-Al_2O_3$ are colinear with the representative point of a pure antigorite. All reactions where chlorite participates may therefore be regarded as a combination of different reactions of the following type:

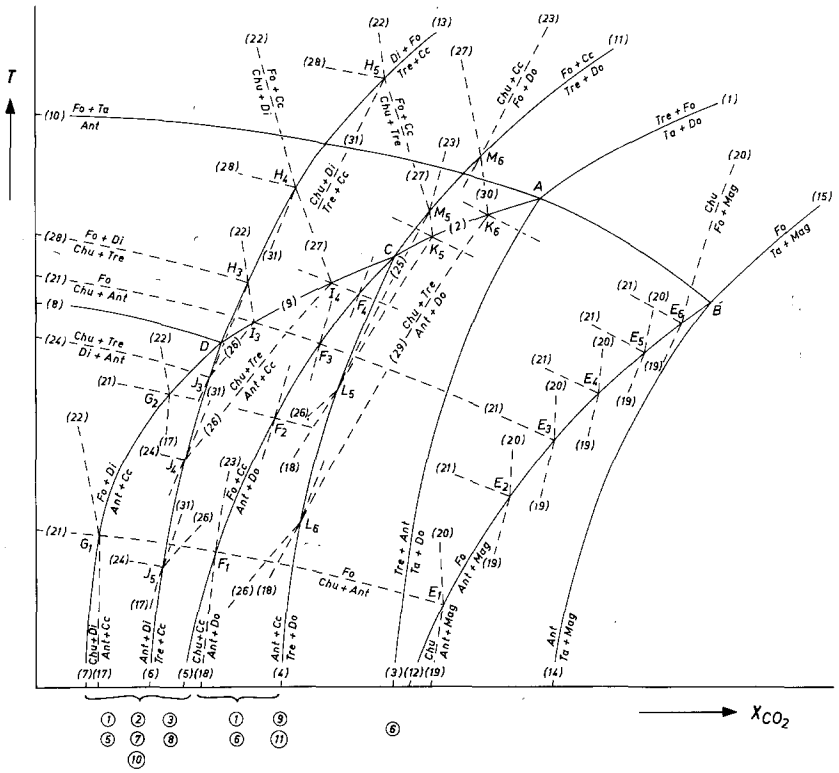

Fig. 8. Petrogenetic grid of the system $CaO-MgO-SiO_2-H_2O-CO_2-HF$ in a $T-X_{CO_2}$-diagram, as derived from observed stable phase assemblages of the Furtschagl marble. Clinohumite absent reactions are drawn with *heavy lines*, reactions with clinohumite are drawn as conturs in six different steps for different F-contents. Total pressure is unknown, but possibly as high as 5 Kbars. *Numbers* in circles below the bottom line are the numbers of the marble lenses, where the corresponding assemblage was found

A + B = antigorite + C

antigorite + chlorite I = chlorite II

A + B + chlorite I = chlorite II + C

with an analogue formation of chlorite III.

Phase relations in the system $CaO-MgO-SiO_2-H_2O-CO_2$ involving serpentine – socalled ophicarbonates – were derived theoretically by Skippen and Trommsdorff (1975) and Trommsdorff and Evans (1977a). Natural examples from Italian alps are given by Trommsdorff and Evans (1972, 1977b).

In order to give a description of phase relations for the mineral phases of the Furtschagl marble, we developed a petrogenetic grid under the assumption that:

(a) antigorite stands for chlorites II and III, because chlorite participates in the reactions only by changing its serpentine component;

(b) clinohumite may be formed beside forsterite if enough HF is available.

Reactions with chondrodite (at a still higher HF-content) are neglected, since chondrodite occurs in one sample only, where no reactions could be observed. For the clinohumite absent reactions the same petrogenetic grid as described by Skippen and Trommsdorff (1975, Fig. 7b) and Trommsdorff and Evans (1977a, Fig. 7, upper part) was found. These reactions depend on the amount of fluorine replacing hydroxyl in (OH)-bearing phases. This effect has been neglected for the sake of simplicity, since the mineral analyses show a generally low F-content for these phases, and it is very likely that this simplification does not produce a large error. Phase relations including clinohumite were derived under the assumption that the clinohumite stability field is limited by the breakdown into forsterite and periclase or forsterite and magnesite. By these reactions several other clinohumite-bearing isobar univariant assemblages are produced. Among these the reactions

$$Chu + Di + CO_2 = Fo + Cc + H_2O \quad (22)$$

$$Chu + Cc + CO_2 = Fo + Do + H_2O \quad (23)$$

are the most important.

Equilibrium conditions for these reactions were calculated by Rice (1979). They lie at increasing X_{CO_2} values as the amount of F substituting for (OH) in clinohumite increases. In the low F-region (which is, therefore, also the low X_{CO_2} region) the two reactions are nearly parallel to the temperature axis. At values for X_F^{chu} (= F/(F + OH) in clinohumite) smaller than 0.5; Rice (1979) gives equilibrium values for X_{CO_2} smaller than 0.2 for reaction (23), reaction (22) is absent. Nevertheless, even at very small X_F^{chu} this reaction (22) can be present. The large uncertainty of the calculated equilibria must be taken into account. With respect to X_{CO_2} – which is most important in this discussion – it is as large as ± 0.25 at 2 Kbars

Table 5. Reactions among the phases forsterite (Mg_2SiO_4), clinohumite ($Mg_9Si_4O_{16}(OH)_2$), diopside ($CaMgSi_2O_6$), tremolite ($Ca_2Mg_5Si_8O_{22}(OH)_2$), talc ($Mg_3Si_4O_{10}(OH)_2$), antigorite ($Mg_{48}Si_{34}O_{85}(OH)_{62}$), calcite ($CaCO_3$), dolomite ($CaMg(CO_3)_2$) and magnesite ($MgCO_3$).

Numbers in the first column correspond to those given in Fig. 8 and in the text; numbers in the last two columns correspond to those given by Rice (1979), and Trommsdorff and Evans (1977)

No.	isobaric univariant assemblages (without F)	Rice	Tr.+Ev.
1	13 Ta + 10 Do = 5 Tre + 12 Fo + 20 CO_2 + 8 H_2O		24
2	40 Do + 13 Ant = 20 Tre + 282 Fo + 383 H_2O + 80 CO_2		6
3	47 Ta + 30 Do + 30 H_2O = 15 Tre + 2 Ant + 60 CO_2		23
4	107 Do + 17 Tre + 107 H_2O = 141 Cc + 4 Ant + 73 CO_2		8
5	20 Do + 1 Ant = 34 Fo + 20 Cc + 31 H_2O + 20 CO_2		1
6	31 Tre + 45 Cc = 107 Di + Ant + 45 CO_2		13
7	20 Cc + 3 Ant = 62 Fo + 20 Di + 93 H_2O + 20 CO_2		3
8	8 Di + 1 Ant = 4 Tre + 18 Fo + 27 H_2O		10
9	40 Cc + 11 Ant = 20 Tre + 214 Fo + 321 H_2O + 40 CO_2		7
10	1 Ant = 18 Fo + 4 Ta + 27 H_2O		0
11	1 Tre + 11 Do = 8 Fo + 13 Cc + 9 CO_2 + H_2O		9
12	20 Mag + Ant = 34 Fo + 31 H_2O + 20 CO_2		1
13	3 Tre + 5 Cc = 11 Di + 2 Fo + 3 H_2O + 5 CO_2	9	14
14	17 Ta + 45 Mag + 45 H_2O = 2 Ant + 45 CO_2		16
15	1 Ta + 5 Mag = 4 Fo + 5 CO_2 + H_2O		17
16	1 Tre + 3 Cc + 2 Qz = 5 Di + 3 CO_2 + H_2O		
	isobaric bivariant assemblages (with F)		
17	14 Ant + 114 Cc = 62 Chu + 114 Di + 382 H_2O + 114 CO_2		(3)
18	4 Ant + 114 Do = 34 Chu + 114 Cc + 114 CO_2 + 90 H_2O		(1)
19	4 Ant + 114 Mag = 34 Chu + 114 CO_2 + 90 H_2O		(1)
20	1 Mag + 4 Fo + 1 H_2O = 1 Chu + 1 CO_2	3	
21	20 Chu + 1 Ant = 114 Fo + 51 H_2O		
22	3 Chu + 1 Di + 1 CO_2 = 14 Fo + 1 Cc + 3 H_2O	14	
23	1 Do + 4 Fo + 1 H_2O = 1 Chu + 1 Cc + 1 CO_2	3	
24	38 Di + 4 Ant = 15 Chu + 19 Tre + 90 H_2O		(10)
25	4 Tre + 52 Do + 4 H_2O = 8 Chu + 60 Cc + 44 CO_2		
26	26 Ant + 114 Cc = 57 Tre + 107 Chu + 642 H_2O + 114 CO_2		(7)
27	11 Chu + 1 Tre + 2 CO_2 = 52 Fo + 2 Cc + 12 H_2O	11	
28	1 Tre + 5 Chu = 24 Fo + 2 Di + 6 H_2O	15	
29	10 Ant + 38 Do = 47 Chu + 19 Tre + 224 H_2O + 76 CO_2		
30	1 Tre + 13 Chu + 4 CO_2 = 60 Fo + 2 Do + 14 H_2O	10	
31	7 Tre + 12 Cc = 1 Chu + 26 Di + 12 CO_2 + 6 H_2O	13	
	isobaric invariant assemblages (without F)		
A:	Tre, Fo, Ta, Do, Ant		
B:	Fo, Ta, Mg, Ant		
C:	Tre, Fo, Cc, Do, Ant		
D:	Di, Fo, Tre, Cc, Ant		
	isobaric univariant assemblages (with F)		
E:	Fo, Chu, Ant, Mg		
F:	Fo, Chu, Ant, Do, Cc		
G:	Fo, Chu, Ant, Di, Cc		
H:	Fo, Chu, Tre, Di, Cc		
I:	Fo, Chu, Tre, Ant, Cc		
J:	Di, Chu, Tre, Ant, Cc		
K:	Fo, Chu, Tre, Ant, Do		
L:	Cc, Chu, Tre, Ant, Do		
M:	Fo, Chu, Trem Do, Cc		

and 650° C. The whole part of the system that is discussed here ranges from 0.0 to 0.2 X_{CO_2} only.

In Fig. 8 a net of phase relations for this region is shown. Clinohumite absent reactions are drawn with heavy lines, reactions with clinohumite are drawn as contours in six steps for six different F-contents. Reactions (22) and (23) are connected with several isobaric univariant curves (labeled E to M) in addition to the isobaric invariant points in the F-free system (labeled A to D). Along these curves

occur the intersection of contours for fixed F-contents in the clinohumite phase with increasing F-content in the sequence 1 to 6, (E_1 to E_6, for example). Other univariant assemblages move with rising F-content from G_1 to G_2 and are then replaced by H_3 to H_6, for instance. Each reaction originating from a point must be connected to the appropriate point that represents the same F-content (reaction (27) from H_5 with reaction (27) from M_5, for example). All reactions and assemblages are compiled in Table 5.

Values for X_F^{chu} in the samples of the marble lenses range from 0.02 to 0.19. Since the observed assemblages are in accordance with this phase diagram, we assume, that this is the range of variation, where this phase diagram is valid.

With this phase diagram (see Fig. 8) the different assemblages can now be described. It will be demonstrated that some of the assemblages plot on the very water rich part of the diagram, others more on the CO_2-rich part. The description follows rising CO_2-contents; in Fig. 7 the representative tetrahedrons are arranged in the same way.

In *lenses Nos. 1, 3, and 5* the stable assemblages, which are represented in Fig. 7a, are Cc–Di–Chl II–Tichu (+Chon in No. 3) and Cc–Do–Fo–Chu–Chl II–Bru in lense No. 5. In lense No. 1 dolomite is present as inclusions in chlorite. Formation of serpentine component is demonstrated by zonation of chlorites and textural relations indicate that it was formed by break down of diopside with forsterite or clinohumite according to reaction (7)

$$Di + Fo + H_2O + CO_2 = Ant + Cc \quad (7)$$

or reaction (17)

$$Di + Chu + H_2O + CO_2 = Ant + Cc \quad (17)$$

or (17′)

$$Di + Chu(Fo) + Chl\ I + H_2O + CO_2 = Chl\ II + Cc. \quad (17')$$

In Fig. 8 these assemblages plot on the very H_2O rich side of the $T-X_{CO_2}$ diagram.

The stable assemblages of *lenses Nos. 2, 7, 8 and 10* are represented in Fig. 7b. No serpentine component was formed, forsterite and clinohumite are stable beside calcite, and in lense No. 10 tremolite is stable beside calcite. This indicates that this assemblage was formed on the water-rich side of reaction (6)

$$Di + Ant + CO_2 = Tre + Cc + H_2O \quad (6)$$

and that the assemblages of lenses Nos. 2, 7, and 8 were formed on the CO_2-rich side of reaction (5)

$$Fo + Cc + H_2O + CO_2 = Do + Ant \quad (5)$$

or (18)

$$Chu + Cc + H_2O + CO_2 = Ant + Do. \quad (18)$$

No relictic minerals or indications for mineral reactions are evident.

In *lense No. 6* and in nodules from *lense No. 1* serpentine (chlorite III) is stable beside dolomite and calcite (see Fig. 7c). Diopside-dolomite is a relictic assemblage. Therefore the stable assemblages must have formed between reactions (5) and (4)

$$Fo + Cc + H_2O + CO_2 = Ant + Do \quad (5)$$
$$Ant + Cc + CO_2 = Do + Tre + H_2O \quad (4)$$

or (18) and (26)

$$Chu + Cc + H_2O + CO_2 = Ant + Do \quad (18)$$
$$Ant + Cc + CO_2 = Tre + Chu + CO_2 + H_2O. \quad (26)$$

In the $T-X_{CO_2}$ phase diagram they plot on a slightly larger X_{CO_2} value than the above mentioned assemblages.

In *lenses Nos. 9 and 11* tremolite is stable beside dolomite, and chlorite III beside calcite and dolomite (see Fig. 7d). Diopside-dolomite is a relictic assemblage. The phases tremolite-serpentine (chlorite III)-calcite-dolomite are stable along reaction (4)

$$Ant + Cc + CO_2 = Do + Tre + H_2O. \quad (4)$$

There is no textural indication that serpentine and calcite react to form dolomite and tremolite. The stability of these four phases together can be explained by the Al_2O_3 content of serpentine.

In the border zone of *lense No. 6* tremolite beside serpentine is decomposed and forms talc and dolomite, see Fig. 7e. There is a clear textural relationship between these phases, as shown in Fig. 6. Formation of talc was nowhere else observed, and tremolites are normally very fresh. The talc-forming reaction (3)

$$Tre + Ant + CO_2 = Ta + Do + H_2O \quad (3)$$

plots on a still higher X_{CO_2} than the above mentioned reactions in the $T-X_{CO_2}$ diagram of Fig. 8.

Discussion

Phase Relations

As stated above the rocks have been influenced by a variscian as well as by an alpine metamorphic event. It is not possible to reconstruct the mineral assemblages formed by the earlier metamorphism. Very probably they included the minerals calcite, dolomite, clinohumite, forsterite, diopside and borate phases. The variety of assemblages in the different marble

lenses, which were formed during the last metamorphism, the reaction rims and the formation of serpentine component can be explained by:

(a) the substitution of F for (OH), changing the stability of hydroxyl bearing phases, especially clinohumite. Fluorine is not distributed equally in all of the marble lenses. Some of them contain large amounts of F-bearing minerals, others, like 9 and 10, don't even show detectable amounts of F in (OH)-bearing phases. Let us assume that the F-content varied by such an amount, that step 4 to 5 (see Fig. 8) is reached. In this case reactions (4), (5), (6), (17), (18), and (26), which describe most of the phase relations of the marble lenses plot in a very narrow region in the $T-X_{CO_2}$ diagram, approximately around the position of reaction (4) and between reactions (5) and (6) in the F-absent phase diagram;

(b) different $X_{CO_2}^{fluid}$ compositions of the marble lenses. The mineral assemblages show an apparent variation in $X_{CO_2}^{fluid}$. The observation of breakdown of tremolite with serpentine to talc and dolomite in the same area where forsterite and calcite are still stable can not be explained by a variation of F content alone. Different $X_{CO_2}^{fluid}$ compositions can be produced by decreasing temperature, starting from relatively high $X_{CO_2}^{fluid}$ compositions and buffering the $X_{CO_2}^{fluid}$ to different values depending on the total composition (mineral assemblage) of the rock. This model implies a retrograde metamorphism. Another possibility is an increase of $X_{CO_2}^{fluid}$, produced by an external reservoir at more or less constant temperatures (i.e., the maximum temperatures of metamorphism). Depending on the permeability of the rocks, their phase assemblage and the amount of fluid phase available, the fluid phase was buffered by different reactions to different values. This model implies a prograde alpine metamorphism, and in fact there is little evidence for a typical retrograde metamorphism in this area. In contrast, decarbonisation reactions took place in the rocks of the Greiner Schiefer series nearby and they possibly represent the external reservoir of CO_2 (and H_2O as well). In addition the formerly An-rich plagioclase of the metatonalites show formation of microliths consisting of carbonate, epidote, and mica, and this supports our view, that these rocks were metamorphosed under conditions, where CO_2 was added during the metamorphism.

Geological Evolution

The marble lenses were deposited as a marine sedimentary carbonate. This is demonstrated by the investigation of oxygen and carbon isotopic ratios by Schoell et al. (1975). The educt of the amphibolite is probably a tuffaceous basaltic rock, since for a normal basic volcanic rock it is too inhomogenous and for a metamorphosed marly sediment the lack of potassium minerals like phlogopite as well as the occurrence of pyropealmandin garnets are not typical. The whole series can be regarded therefore as a metamorphosed tuffaceous rock with intercalated siliceous dolomitic limestone and (very subordinately, see lense No. 11) quartzitic layers.

The *first metamorphism* must have taken place before the intrusion of the tonalitic plutons. This is demonstrated by the observation, that the pegmatitic dikes contain xenoliths of amphibolite with a clearly developed schistosity. If the plutonic rock had intruded into a sediment, hornfelses instead of amphibolite should be served. The age of this metamorphism must be early variscian or prevariscian.

The *second metamorphism* was induced by the intrusion of the variscian tonalitic rocks and accompanied by a metasomatism. At this time the minerals chlorite I, forsterite, clinohumite (chondrodite) and diopside were formed, or, if they had been already formed by the earlier regional metamorphism, remained stable. Boron metasomatism produced ludwigite and karlite in the SiO_2-poor marble and turmaline in the amphibolite. Very likely fluorine was also introduced during this stage, since near to the contact to the metatonalite F-bearing clinohumite is an important constituent of the marble. The marble lenses further away from the contact, lack any considerable amount of F-substitution in (OH) bearing minerals. Pegmatitic dikes intruded into the amphibolite at this stage and the garnets of the amphibolite obtained a grossular rich rim. This indicates rather high temperatures, but no exact $P-T$-data can be given.

The last observable event was the *alpine metamorphism*. Within the marble lenses this metamorphism produced serpentine component (as chlorite II and III) by the breakdown of some of the clinohumite, forsterite, and diopside of the earlier assemblage. Nevertheless, at suitable conditions ($X_{CO_2}^{fluid}$, $X_F^{mineral}$) these three phases are still stable. It is impossible to decide at what times the tremolite of the marble was formed. Tremolite is stable over a wide range of pressures and temperatures, and it may be a product of the earliest regional metamorphism, unchanged by the following ones, as well as a product of the last alpine event. The observation that tremolite is present only in marble lenses further away from the contact to the tonalite may, then, represent a contact metamorphism isograd, but it may also be due to the low F-content of these assemblages.

Since the last metamorphism is marked by volatile consuming reactions in this already metamorphosed (=volatile poor) rock series, there is no proof that the condition $P_f = P_s$ is valid for this occurrence. Therefore it is difficult to derive exact data for the

$P-T$-conditions of the last metamorphism. Temperatures of about 600° C (Hoernes and Friedrichsen 1974) from $^{16}O/^{18}O$-data as well as a minimum pressure of about 5 kbars (Hoschek 1979) are in accordance with the mineral assemblage observed here.

Acknowledgements. The authors would like to thank G. Morteani and E. Koch for their assistance during the field trips. P. Metz, G. Morteani, G. Hoschek, J.M. Rice, and V. Trommsdorff critically read the manuscript, and B.W. Evans and J.M. Rice provided unpublished data. Special thanks are due to P.M. Orville for many helpful discussions. C. Dietsch kindly corrected the English version. Field work was supported by a grant from the Deutsche Forschungsgemeinschaft, microprobe work by the Stiftung Volkswagenwerk.

References

Ackermand D, Morteani G (1976) Kontinuierlicher und diskontinuierlicher Zonarbau in den Granaten der penninischen Gesteine der Zillertaler Alpen (Tirol/Österreich). Tschermaks Mineral Petrogr Mitt 23:117–136

Angenheister G, Bögel H, Gebrande H, Giese P, Schmidt-Thomé P, Zeil W (1972) Recent investigations of surficial and deeper crustal structures of the eastern and southern alps. Geol Rundsch 61:349–395

Aoki K, Fujino K, Akaogi M (1976) Titanchondrodite and titanclinohumite derived from the upper mantle in the Buell Park kimberlite, Arizona, USA. Contrib Mineral Petrol 56:243–253

Borg IY, Smith DK (1969) Calculated X-ray powder patterns for silicate minerals. Geol Soc Am Mem 122: Boulder/Colorado

Brown G (1961) The X-ray identification and crystal structures of clay minerals. Mineral Soc London, XI:544 p.

Christa E (1931) Das Gebiet des oberen Zemmgrundes in den Zillertaler Alpen. Jahrb Geol Bundesanst (Austria) 81:3/4, 534–636

Cliff RA (1971) The age of tonalites in the south-east Tauernfenster, Austrian Alps – Rb/Sr whole rock ages on some associated leucogranites. Neues Jahrb Geol Paleontol Monatsh 1971:655–669

Deer WA, Howie RA, Zussman J (1962) Rock-forming minerals, vol 3, Sheet silicates. Longman, London

Deer WA, Howie RA, Zussman J (1963) Rock-forming minerals, vol 2, Chain silicates. Longman, London

Franz G, Ackermand D, Koch E (1980) Karlite, $Mg_7(BO_3)_3(OH, Cl)_5$, a new borate mineral and associated Ludwigite from the eastern alps. Am Mineral (in preparation)

Fujino K, Takeachi Y (1978) Crystal chemistry of titan-chondrodite and titan-clinohumite of high pressure origin. Am Mineral 63:535–543

Gold DP (1966) The minerals of the Oka carbonatite and alkali complex, Oka, Quebec. Mineral Soc India, IMA vol (IMA Papers and Proc 4th gen meeting, New Delhi, 1964) 109–125

Goldsmith JR, Graf DL, Joensuu OJ (1955) The occurrence of magnesian calcite in nature. Geochim Cosmochim Acta 7:212–230

Hinthorne JR, Ribbe PH (1974) Determination of boron in chondrodite by ion microprobe mass analysis. Am Mineral 59:1123–1126

Hoernes S, Friedrichsen F (1974) Oxygen isotope studies on metamorphic rocks of the western Hohe Tauern (Austria). Schweiz Mineral Petrol, Mitt 54:769–788

Hoschek G (1979) Metamorphose kalkiger Metasedimente in den westlichen Hohen Tauern. Fortschr Mineral 57 (1):45

Jones NW, Ribbe PH, Gibbs GV (1969) Crystal chemistry of the humite minerals. Am Mineral 54:391–411

Magnusson NH (1940) The Herräng field and it's iron ores. Åresbok Sveriges Geol Undersökning 34 (1):1–72

Morteani G (1974) Petrology of the Tauern Window, Austrian Alps. Fortschr Mineral 52 (1):195–220

Ribbe PH (1979) Titanium, hydroxyl and fluorine in the humite minerals. Am Mineral 64:1027–1035

Rice JM (1980) Phase equilibria involving humite minerals in impure dolomitic limestones. Part I: Calculated stability of clinohumite. Contrib Mineral Petrol 71:219–235

Sander B (1911) Geologische Studien am Westende der Hohen Tauern (1. Bericht). Denkschr Akad Wiss Wien, Math Nat Kl 82:257–319

Schoell M, Morteani G, Hörmann PK (1975) $^{18}O/^{16}O$ and $^{13}C/^{12}C$ ratios of carbonates from gneisses, serpentinites and marbles of the Zillertaler Alpen, western Tauern Area (Austria). Neues Jahrb Mineral Monatsh 10:444–459

Shaw DM, Moxham RL, Filby RH, Lapkowsky WW (1963) The petrology and geochemistry of some Grenville skarns. Part II: Geochemistry. Can Mineral 7:578–616

Skippen G, Trommsdroff V (1975) Invariant phase relations among minerals on $T-X_{fluid}$ sections. Am J Sci 275:561–572

Tilley CE (1951) The zoned contact-skarns of the Broadford Area, Skye: A study of boron-fluorine metasomatism in Dolomites. Mineral Mag 29:621–666

Trommsdorff V, Evans BW (1972) Progressive metamorphism of antigorite schist in the Bergell Tonalite Aureole (Italy). Am J Sci 272:423–437

Trommsdorff V, Evans BW (1977a) Antigorite-ophicarbonates: Phase relations in a portion of the system $CaO-MgO-SiO_2-H_2O-CO_2$. Contrib Mineral Petrol 60:39–56

Trommsdorff V, Evans BW (1977b) Antigorite-ophicarbonates: Contact metamorphism in Valmalenco, Italy. Contrib Mineral Petrol 62:301–312

Trommsdorff V, Evans BW (1980) Titan hydroxyl-clinohumite: Formation and breakdown in antigorite rocks (Malenco, Italy). Contrib Mineral Petrol 72:229–242

Received May 8, 1980; Accepted September 19, 1980